

---

# OUT-OF-DISTRIBUTION PARTIAL LABEL LEARNING

---

**Jintao Huang, Yiu-Ming Cheung and Chi-Man Vong**

Department of Computer Science, Hong Kong Baptist University, Hong Kong, China, SAR.  
Department of Computer and Information Sciences, University of Macau, Macau, China, SAR.

## ABSTRACT

Partial Label Learning (PLL) tackles model learning from the data with inexact labels under the assumption that training and test objects are in the same distribution, i.e., closed-set scenario. Nevertheless, this assumption does not hold in real-world open-set scenarios where test data may come from Out-Of-Distribution (OOD), resulting in object detection failure and hence significantly compromising the PLL model’s security and trustworthiness. This is a previously unexplored problem called Out-Of-Distribution Partial Label Learning (OODPLL) that our newly proposed PLOOD framework can effectively resolve. During the training phase, our framework leverages self-supervised learning strategy to generate positive and negative samples for each object, emulating in and out-of-distributions respectively. Under these distributions, PLL methods can learn discriminative features for OOD objects. In the inference phase, a novel Partial Energy (PE) scoring technique is proposed which leverages the label confidence established during the above training phase to mine the actual labels. In this way, the issue of inexact labeling in PLL can be effectively addressed for significantly better performance in OOD object detection. PLOOD is compared with SOTA PLL models and OOD scores on CIFAR-10 and CIFAR-100 datasets against various OOD datasets. The results demonstrate the effectiveness of our PLOOD framework, significantly outperforming SOTA PLL models and marking a substantial advancement in addressing PLL problems in real-world OOD scenarios.

## 1 Introduction

Partial label learning (PLL) [13, 9, 18] is a form of weakly supervised learning where each sample is associated with a set of candidate labels, among which only one is correct. PLL effectively avoids the burden for precise annotation and hence significantly reduces labeling costs [17]. PLL aims to develop noise-tolerant multi-class classifiers by identifying the ground-truth label from the candidate labels and is adaptable across various domains like image annotation, web mining, and ecological informatics [11, 5, 21, 6]. Due to the low annotation costs and the addressability on the challenging label ambiguity, PLL has become a crucial area in artificial intelligence research and is promising to enhance model efficiency and applicability in real-world scenarios.

Despite PLL methods being widely utilized across various fields, they do come with notable limitations. These techniques are all grounded on the closed-set assumption, which necessitates that all test instances adhere to the same distribution as the training data. Nevertheless, this assumption does not hold in practical applications. In reality, out-of-distribution (OOD) instances are always encountered [14, 1, 23, 4] that deviate significantly from the training set distribution during predictions. Since a trained model can only classify the OOD instances into existing categories, a substantial decline in classification performance is resulted. Moreover, the OOD instances potentially disrupt the model’s learning process, putting its security and trustworthiness at risk. This presents significant challenges for PLL learning and underscores the limitations of current PLL methods in addressing the issues posed by OOD instances. Although it is crucial to incorporate OOD scenario into PLL, it has not yet been studied..

This paper formalizes this learning scenario into a new problem called Out-Of-Distribution Partial Label Learning (OODPLL). Figure 1 shows a practical case of OODPLL in scenarios such as animal image classification. The primary objective of OODPLL is to address the challenge of PLL in effectively detecting OOD objects and accurately classifying objects within the distribution. Integrating existing OOD techniques with PLL methods offers a potential solution to

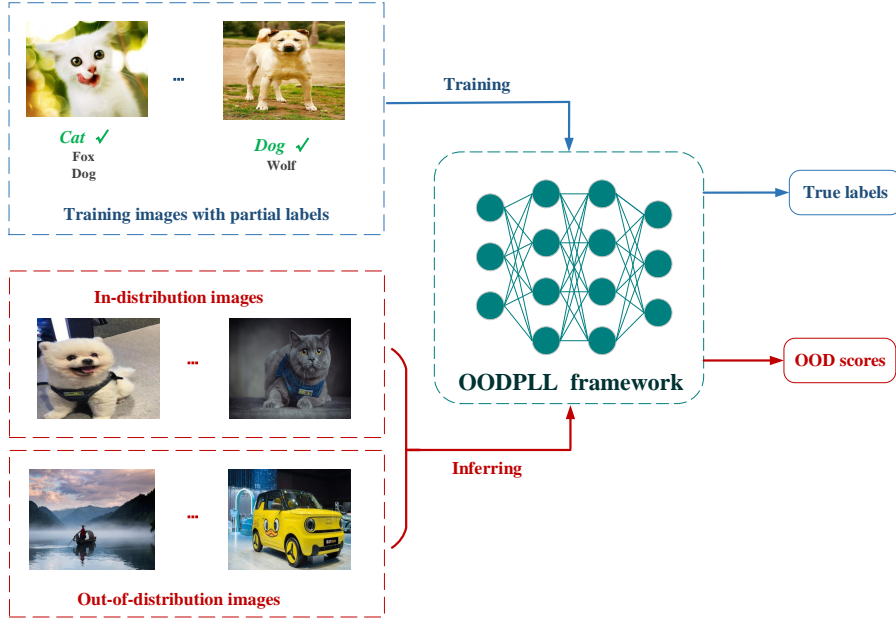


Figure 1: An example of OODPLL. (Top-left) A scenario of animal image classification for training. Each image has a set of candidate labels, such as (Cat, Fox, and Dog) but only Cat is the true label. (Bottom-Left) Animal images of in-distribution (ID) and OOD. In such cases, the OODPLL task needs to both identify the true labels of the animals (iID objects) and detect the non-animal category (i.e., OOD objects).

the OODPLL but introduces two challenging problems: 1) Existing PLL models are not trained on negative examples (i.e., OOD objects). Without learning the features of OOD objects, the PLL models fail to effectively differentiate the in-distribution (ID) and OOD objects. 2) Despite the effectiveness of OOD detection strategies in supervised learning [19], the inexact labeling ambiguity in PLL can lead to incorrect weighting of ID and OOD objects [15]. This mis-weighting causes ID samples misidentified into OOD anomalies or vice versa, significantly reducing the model performance. From these two challenges, it reveals the crucial need for a new approach to address the intricate issues of OODPLL.

This paper proposes a novel framework, PLOOD, designed to address the issue of OODPLL effectively. The framework comprises a Self Supervised-based Feature representation Enhancement module (SSFE) and a novel Partial Energy-based (PE) OOD detection module. Given that the inexact supervised information of PLL grapples to guide the identification of OOD samples, the SSFE module initially generates various rotated objects for the training samples of PLL based on self-supervised learning [8]. Inspired by Positive Unlabeled (PU) learning [7, 2], the original images in the dataset are considered positive examples, while the unlabeled examples, including all rotated copies, are negative ones. In this way, the SSFE module emulates the learning of both ID and OOD samples in PLL, thus significantly enhancing the feature representation capability of PLL models. Following this, the advanced feature representation acquired from SSFE is fine-tuned to enable the PLL to acquire the necessary features for identifying inexact labels. More precise supervision information is attained by progressively adjusting the label confidence matrix to ultimately address the issue of candidate labels with inexact supervised information. Simultaneously, our newly proposed PE module utilizes the energy model framework [12] for the calculation of OOD weights. By leveraging the label confidence obtained from the SSFE module, the misidentification issue caused by inexact PLL labeling during training can be mitigated. By combining label confidence containing effective label correlation of ID samples, the PE module effectively guides PLL in the OOD detection stage, enhancing the weight of ID samples and reducing the weight of OOD samples, thereby significantly improving OOD detection accuracy. Through these innovative modules, the PLOOD framework effectively addresses the challenges of OODPLL.

**Motivations and Contributions:** Despite the prevalent usage in various domains, existing PLL methods face a critical challenge, notably their dependency on the closed-set assumption, which is often violated by OOD instances in practical applications. This violation significantly degrades PLL model performance, security, and trustworthiness. In this paper, a new OODPLL task is introduced, and a corresponding solution framework called PLOOD is proposed to tackle the issue of detecting and classifying the OOD objects within PLL frameworks. Our PLOOD integrates an SSFE

module and a PE OOD detection module. The SSFE module leverages self-supervised learning to generate rotated positive and negative (OOD) objects for the training of PLL models over both ID and OOD samples, enhancing the feature representation capability of PPL models. Meanwhile, the PE module improves OOD detection accuracy by combining label confidence with supervision information. This approach successfully addresses the critical challenges of OODPLL, offering a significant advancement for the PLL community in handling OOD objects.

## 2 Proposed Methodology

We assume a PLL training datasets with  $N$  same distribution samples  $\mathbf{D} = \{(\mathbf{x}_i, \mathbf{y}_i) | 1 < i < N\}$ , and its corresponding feature space and label space are  $\mathbf{X} \in R^d$  and  $\mathbf{L} = \{0, 1\}^q$  where  $q$  is the number of candidate labels, respectively. Given testing datasets containing ID samples and OOD samples simultaneously, the task of OODPLL is to induce a multi-class classifier  $f : \mathbf{X} \rightarrow \mathbf{L}$ , which can effectively detect the OOD samples and precisely predict the ground-truth label of the unseen ID samples.

The proposed PLOOD method is designed to address the OODPLL problem effectively. Unlike existing PLL methods that are unable to learn OOD features, PLOOD incorporates a Self Supervised-based Feature representation Enhancement (SSFE) module. By utilizing PU learning [7] and predicting rotated positive and negative examples, PLOOD’s capacity to differentiate OOD samples is significantly improved. Additionally, the label confidences in solving inexact labeling are learned from fine-tuned SSFE module. Furthermore, unlike the current OOD detection scores, the newly proposed Partial Energy (PE) OOD detection score in PLOOD integrates the label confidence acquired from the SSFE module with the energy score. PE significantly induces the model to mitigate the errors stemming from inexact supervision information in PLL, thereby enhancing the model’s detection capability and effectively resolving the OODPLL problem.

### 2.1 SSFE Module with Predicting Positive and Negative Rotated Objects

In a training dataset  $\mathbf{D}$  consisting of objects  $\{\mathbf{x}_i\}_{i=1}^N$ , SSFE modules firstly generates rotational transformation  $G = \{g(\mathbf{x}_i; r)\}_{r=1}^R$  where  $R$  is the number of rotated objects for each  $\mathbf{x}_i$ . Under rotation by a certain degree, each  $\mathbf{x}_i$  becomes  $\mathbf{x}_{i,r} = g(\mathbf{x}_i; r)$ . In the SSFE module, the original image is considered as a positive example. In contrast, all rotated examples (even the ones without labels) are treated as negative, which helps PLOOD to learn the distinguishing features between ID and OOD samples. This approach effectively turns the rotation detection problem into a binary classification problem. Each rotated image is assigned a weight based on the estimated probability, and this helps reduce the relative loss of rotated negative samples.

**Rotation Classification Loss:** PLOOD utilizes a ResNet model to train for binary classification. Each rotated image  $\mathbf{x}_i$  is processed through the feature extractor  $E$  to generate high-level feature representation  $h_i^{RC}$ ; subsequently, the classifier  $f$  maps these features to logits:  $f : h_i^{RC} \rightarrow t^r(x_i^r)$  where the logit vector is derived as  $t(x_i^r) = f(E(x_i^r))$ , the probability  $P^r(x_i^r)$  of estimating  $\mathbf{x}_i$  is denoted as:

$$P^r(\mathbf{x}_i^r) = \frac{\exp(t(x_i^r))}{\sum_{j=1}^R \exp(t_j^r(x_i^r))}. \quad (1)$$

A weight for each instance is introduced into the cross-entropy loss  $\ell_{CE}$ . Therefore, the rotation classification loss function can be denoted as:

$$\ell_{RC}(\theta) = -\frac{1}{N \times R} \sum_{i=1}^N \sum_{r=1}^R w_{i,r} \ell_{CE}(P^r(\mathbf{x}_i^r), \mathbf{z}_i^r), \quad (2)$$

where  $\mathbf{z}_i^r$  is the correct rotational label, and

$$w_{i,r} = \begin{cases} 1 & r = 1, \\ 1 - P^r(\mathbf{x}_i^r) & \text{otherwise.} \end{cases} \quad (3)$$

**Rotation Irrelevance Loss:** Despite optimizing (2) enables PLOOD to learn how to distinguish OOD, the rotation of each sample is essentially identically distributed to a certain extent. Therefore, to effectively reduce the error caused by the rotation of the same sample in practical scenarios, we ensure that the features of the same image under different rotation degrees are similar, resulting in rotation-invariant features. Specifically, we aim to make the respective features of a set of rotated copies of an image highly similar. To achieve this, we minimize the distance between each feature

$\{h_r^{RI}\}_{r=1}^R$  and its average feature vector  $\bar{h} = \frac{1}{R} \sum_{r=1}^R h_r^{RI}$ . The rotation irrelevance loss function is written as:

$$\ell_{RI}(\theta) = \frac{1}{N \times R} \sum_{i=1}^N \sum_{r=1}^R d(h_{i,r}^{RI}, \bar{h}_i), \quad (4)$$

where  $d(h_{i,r}^{RI}, \bar{h}_i)$  is one of the distance computation metric.

Consequently, the SSFE module incorporates two loss functions, (2) and (4), for optimization:

$$\ell_{SSFE}(\theta) = \alpha \ell_{RC}(\theta) + (1 - \alpha) \ell_{RI}(\theta), \quad (5)$$

where  $\alpha$  is the trade-off parameters between  $\ell_{RC}(\theta)$  and  $\ell_{RI}(\theta)$ , and  $\alpha = 0.5$  is used in our experiment.

With the SSFE module, PLOOD acquires the ability to learn the feature representation  $h^{RC}$  effectively distinguishing rotation (thus differentiating OOD), and the rotation-irrelevance features  $h^{RI}$ . These two features are integrated to obtain feature representation of SSFE as  $H_{SSFE}$ , which is then employed to provide additional guidance to PLL in addressing the challenges related to inexact labeling ambiguity.

## 2.2 Addressing Partial Label Ambiguity by Label Confidence with SSFE module

SSFE provides PLOOD with the ability to distinguish OOD samples, and PLOOD also needs the ability to learn to distinguish inaccurately labeled features. For each image  $\mathbf{x}_i$  with partial label set  $\mathbf{Y}_i = \{\mathbf{y}_{i,j}\}_{j=1}^q$ , the  $H_{SSFE}$  is finetuned to train a new feature extractor  $E^*$ , which learns a new feature representation  $H_{PL}^*$  that unravels the issue of inexact labels by optimizing the following partial label loss function:

$$\ell_{PL}(\theta^*) = -\frac{1}{N} \sum_{\mathbf{x}_i \in \mathbf{X}} \sum_{\mathbf{y}_j \in \mathbf{Y}} \mathbf{C}(\mathbf{x}_i; \mathbf{y}_j) \times \ell_{CE}(P_j^*(\mathbf{x}_i), \mathbf{y}_{i,j}), \quad (6)$$

where  $P_j^*(\mathbf{x}_i)$  represents the probability assigned by the model to label  $\mathbf{y}_j$  for instance  $\mathbf{x}_i$  induced by the logits:  $t^*(\mathbf{x}_i) = f^*(E^*(\mathbf{x}_i))$ . And  $\mathbf{C}(\mathbf{x}_i; \mathbf{y}_j)$  denotes the label confidence associated with label  $\mathbf{y}_j$  for instance  $\mathbf{x}_i$  where it is initialized by normalizing the partial labels.  $\mathbf{C}(\mathbf{x}_i; \mathbf{y}_j)$  can be dynamically updated as the model trains, and the updating after each training iteration is formulated as follows:

$$\mathbf{C}(\mathbf{x}_i; \mathbf{y}_j)^{t+1} = \mathbf{C}(\mathbf{x}_i; \mathbf{y}_j)^t \otimes \text{softmax}(P_j^*(\mathbf{x}_i)). \quad (7)$$

Ultimately, the disambiguated label confidence matrix  $\mathbf{C}$  effectively recognizes the actual label within the PLL candidate label set, thereby resolving the issue of inexact supervised information. In the subsequent OOD detection task, we incorporated the labeling confidence matrix to prevent PLOOD from being influenced by mis-weighting resulting from inexact labeling.

## 2.3 Partial-Energy Score-based OOD Detection

The Partial-Energy (PE) score is based on the Energy-based models [12] to understand data distribution in terms of energy levels. Lower energy levels represent data configurations more likely to be in distribution (ID), while higher energy levels suggest potential OOD samples. This section provides a comprehensive examination of the approach, delving into its theoretical foundations, practical implementation, and the essential role of aggregate label confidence ( $G_{LC}$ ) in refining the detection mechanism.

### 2.3.1 Aggregate Label Confidence and Calibration

$G_{LC}$  presents a nuanced approach for refining OOD detection strategies within PLL by leveraging the comprehensive performance metrics obtained during the model’s training on ID data. This section explains the sophisticated mechanisms involved in deriving  $G_{LC}$ , outlining its formulation, calibration process, and critical role in enhancing the model’s ability to differentiate between ID and OOD instances.

Initially, the label confidence matrix  $\mathbf{C}$  can be obtained from the ID training process by Equation (7). Each entry in the matrix  $\mathbf{C}$  reflects the confidence or reliability of the model in predicting the specific label  $\mathbf{y}_j$ , typically measured through the proportion of correct predictions. Defined as the arithmetic mean of all label confidence scores,  $G_{LC}$  provides a global measure of the model’s prediction reliability across its label spectrum, which is formally defined as:

$$G_{LC}(\mathbf{y}_j) = \frac{\mathbf{C}(\mathbf{X}; \mathbf{y}_j) - \mu_{\mathbf{y}_j}}{\sigma_{\mathbf{y}_j}}, \quad (8)$$

where  $\mu_{\mathbf{y}_j}$  is the mean scores of label  $\mathbf{y}_j \in \mathbf{Y}$  across all ID samples, and  $\sigma_{\mathbf{y}_j}$  is variance of label  $\mathbf{y}_j$ , which are defined as:

$$\mu_{\mathbf{y}_j} = \frac{1}{N} \sum_{\mathbf{x}_i \in \mathbf{ID}} \mathbf{C}(\mathbf{x}_i; \mathbf{y}_j), \quad (9)$$

$$\sigma_{\mathbf{y}_j} = \sqrt{\frac{1}{N} \sum_{\mathbf{x}_i \in \mathbf{ID}} (\mathbf{C}(\mathbf{x}_i; \mathbf{y}_j) - \mu_{\mathbf{y}_j})^2}. \quad (10)$$

$G_{LC}$  is an essential component of the PLL framework, as it greatly enhances its ability to detect OOD examples. By utilizing a model’s aggregated performance metrics from in-distribution (ID) training,  $G_{LC}$  ensures that the OOD detection mechanism reflects the model’s predictive reliability and is adaptable to its label-specific confidence levels. This strategic calibration fosters a nuanced and data-informed approach to distinguishing between ID and OOD instances, significantly improving the model’s performance in complex learning environments.

### 2.3.2 Adjusted Partial Energy Score for PLL-OOD Detection

Energy-based models are a way of conceptualizing data distribution by assigning energy levels to different data configurations [12]. The lower the energy level, the more typical the configuration is of ID data, while higher energy levels suggest configurations that deviate significantly and may signal potential OOD instances. The energy function, often calculated from the model’s logits, is crucial in distinguishing between these configurations. The PE score is a significant metric within the PLOOD detection framework. It aims to measure the degree to which an instance aligns with the model’s learned distribution and can indicate potential OOD instances. What distinguishes the PE score is its ability to account for ambiguity in partially labeled instances by integrating  $G_{LC}$  into the energy-based score.

Given an instance  $\mathbf{x}_i$  with a set of candidate labels  $\mathbf{y}_j$ , the Partial-Energy Score  $PE(\mathbf{x}_i)$  is computed by adjusting the energy score for each candidate label  $\mathbf{y}_j$  with the corresponding label confidence  $\mathbf{C}(\mathbf{x}_i; \mathbf{y}_{i,j})$ , reflecting the instance’s OOD probability:

$$PE(\mathbf{x}_i) = \sum_{\mathbf{y}_j \in \mathbf{Y}} G_{LC}(\mathbf{y}_j) \times E(\mathbf{x}_i; \mathbf{y}_{i,j}), \quad (11)$$

where  $G_{LC}(\mathbf{y}_j)$  acts as a weighting factor, reflecting the model’s confidence in its prediction for  $\mathbf{y}_j$ , and  $E(\mathbf{x}_i; \mathbf{y}_{i,j})$  signifies the energy associated with label  $\mathbf{y}_j$  for instance  $\mathbf{x}_i$ :

$$E(\mathbf{x}_i; \mathbf{y}_j) = -\log(1 + \exp(P_j^*(\mathbf{x}_i))), \quad (12)$$

where  $P_j^*(\mathbf{x}_i)$  is consistent with Equation (6). The PE can be interpreted from likelihood perspective:

$$\begin{aligned} E(\mathbf{x}_i; \mathbf{y}_j) &= \sum_{j=1}^q G_{LC}(\mathbf{y}_j) \times \log(p(\mathbf{x}_i | \mathbf{y}_{i,j} = 1) \cdot Z_{\mathbf{y}_{i,j}}) \\ &= G_{LC}(\mathbf{y}_j) \times \left( \sum_{j=1}^q \log p(\mathbf{x}_i | \mathbf{y}_{i,j} = 1) + Z \right), \end{aligned} \quad (13)$$

where  $p(\mathbf{x}_i | \mathbf{y}_{i,j} = 1) = \frac{e^{\log(1+P_j^*(\mathbf{x}_i))}}{\int_{\mathbf{x}_i | \mathbf{y}_{i,j}} e^{\log(1+P_j^*(\mathbf{x}_i))}}$  is the conditional likelihood, and  $Z = \sum_{j=1}^q \log Z_{\mathbf{y}_{i,j}}$  where  $Z_{\mathbf{y}_{i,j}} = \int_{\mathbf{x}_i | \mathbf{y}_{i,j}} e^{\log(1+P_j^*(\mathbf{x}_i))}$  is the normalized density.

Integrating  $G_{LC}$  into the energy-based detection process significantly improves OOD detection in the PLL framework. This method leverages the model’s predictive ability incorporated with label confidence solving the inexact labeling, offering a more reliable and effective way to identify OOD instances. This approach boosts OOD detection effectiveness and enhances the PLOOD framework’s overall performance.

## 3 Experiments

The PLOOD framework has been thoroughly evaluated to showcase its precision in accurately classifying ID data while adeptly identifying and handling OOD instances. This section presents a comprehensive overview of the experimental setup, the results, and the implications and insights gleaned from the comparative studies.

### 3.1 Experimental Setup

**Dataset Selection:** The choice of datasets is crucial in assessing the robustness, adaptability, and accuracy of the PLOOD framework in distinguishing between **ID** and **OOD** data. **ID datasets:** In evaluating the framework’s performance, we utilize **CIFAR-10** and **CIFAR-100** as ID datasets. CIFAR-10 consists of 60,000 images spanning ten categories to test the model’s generalization capabilities, while CIFAR-100 presents 100 categories to challenge the model’s differentiation abilities further. **OOD datasets:** In OOD evaluation, our framework is tested against various datasets, including FashionMNIST (Fashion), the Describable Textures Dataset (DTD), LSUNCrop (LSUN), TinyImageNetCrop (Tiny), and Fooling Images (Fooling), which represent diverse domains such as environmental, architectural, and object scenes.

**Comparing Method:** We have chosen the SOTA PLL algorithm PaPi [16] and CAVL [20] to assess PLL through OOD detection techniques fairly and effectively. We have combined our approach with existing OOD detection methods to enhance it further. The PaPi and CAVL are the deep-based PLL models with a guided prototypical classifier, while the detection methods we incorporated include Entropy [3], ODIN [10], DML [22], EnergyBased [12], and JointEnergy (J.Energy) [15].

**Evaluation Metrics:** Our approach was evaluated using two commonly used OOD evaluation metrics: Area Under the Precision-Recall Curve for In-distribution (AUPR-IN) and False Positive Rate at 95% True Positive Rate (FPR95).

**Training Details:** The PaPi, CAVL, and PLOOD models all utilize the ResNet34 architecture as the backbone, with a learning rate set at  $1e-3$  and gradually adjusted based on decay. A batch size of 128 is used, and the Adam optimizer is selected for its adaptive learning rate feature, with a standard parameter having a momentum of 0.9. The training process spans 100 epochs, with a widened factor of 2 and a drop rate of 0.3. The experiments were carried out on a Windows 13th Gen Intel(R) Core(TM) i7-13700K 3.40 GHz with NVIDIA GeForce RTX 4080, 32GB RAM, and PyTorch environments.

### 3.2 Experimental Results

#### 3.2.1 Comparisons between PLOOD and Existing Intergraded Framework (SOTA PLL methods + OOD detection scores)

The emergence of OODPLL as a new research problem means that there is currently no SOTA method to directly compare with the proposed PLOOD algorithm. To thoroughly and fairly evaluate the effectiveness of the PLOOD framework, we conducted a comparison against two existing SOTA PLL methodologies using five widely recognized OOD metrics. The results, presented in Tables 1 and 2, clearly demonstrate that the PLOOD framework exhibits superior performance across CIFAR-10 and CIFAR-100 datasets with five OOD detection datasets. Specifically, Table 1 shows that compared to the PaPi algorithm integrated with the five OOD metrics, the AUPR-IN of PLOOD on the five OOD detection datasets increased by 6.19% to 20.41% and 6.33% to 14.41%, respectively, with enhancements of 7.58% to 23.95%, 10.42% to 11.86%, and 10.53% to 21.1%. Compared to the CAVL algorithm, PLOOD demonstrated improvements of 11.22% to 25.03%, 8.51% to 13.79%, 13.11% to 23.01%, 9.14% to 18.57%, and 9.94% to 15.93%, respectively.

Concerning the FPR95 metric, PLOOD’s advancements on the Tiny OOD dataset were markedly pronounced. Against the PaPi and CAVL algorithms, enhancements of 9.87% to 22.45% and 13.62% to 23.81% were observed, respectively. These outcomes unequivocally indicate that PLOOD’s superiority primarily stems from the adept OOD feature differentiation capability intrinsic to the SSFE module, a capability conspicuously absent in the current PaPi and CAVL algorithms. The SSFE module further induces PLLs with the proficiency to discern and progressively disambiguate inexact labels. Concurrently, the integration of Parietal Energy (PE) with the label confidence matrix markedly mitigates the mislabeling issue engendered by label ambiguity, thereby significantly enhancing OOD detection performance. It is noteworthy that the overall performance of the PaPi method surpasses that of the CAVL algorithm. Within the ambit of the five OOD metrics, Energy-based metrics manifest superior performance relative to other metrics. This observation is corroborated in Table 2. In summation, PLOOD establishes a novel benchmark in OOD detection within the PLL domain. Its innovative methodology of amalgamating label confidence with energy score computations positions PLOOD as an effective and reliable framework in intricate open-close set scenarios.

#### 3.2.2 Ablation Experiments on SSFE Module and PE Module of PLOOD

To further verify the impact of the two modules SSFE and PE on proposed PLOOD framework, we conducted the following two ablation experiments.

Table 1: Performance comparisons of the **PLOOD** framework and **two existing PLL methods with five OOD scores** on the **five OOD datasets** of **CIFAR-10** under partial rate ( $p = 0.1$ ). **AUPR-IN(%)** and **FPR95(%)** are used for the evaluation. The underline indicates the optimal result of the current PLL method, and the bolded font is the optimal result of all cases.

Metrics		AUPR-IN ( $\uparrow$ ) / FPR95 ( $\downarrow$ )				
PLL methods	OOD scores	Fashion	LSUN	Tiny	DTD	Fooling
PaPi [16]	ODIN [10]	56.20/86.37	67.95/80.55	55.13/91.62	53.95/93.09	67.10/89.31
	DML [22]	66.05/77.10	72.58/76.06	68.46/82.17	53.90/90.77	56.74/95.69
	Entropy [3]	<u>70.41/74.79</u>	67.39/79.69	64.47/84.35	52.67/92.18	65.41/88.68
	Energy [12]	67.14/77.12	75.08/73.76	70.86/82.21	<u>55.09/88.31</u>	67.15/85.32
	J.Energy [15]	68.98/75.48	<u>76.65/72.08</u>	<u>71.50/79.04</u>	54.11/89.01	<u>67.31/85.01</u>
CAVL [20]	ODIN [10]	51.57/88.67	70.57/88.20	56.07/92.98	45.96/97.86	62.61/89.61
	DML [22]	65.21/82.46	69.19/89.98	65.81/84.52	50.53/93.10	61.91/90.18
	Entropy [3]	65.13/81.81	70.22/85.54	65.86/83.88	51.01/91.46	62.48/89.47
	Energy [12]	<u>65.38/80.46</u>	<u>74.47/79.01</u>	<u>65.97/83.77</u>	54.69/88.10	62.94/90.18
	J.Energy [15]	62.64/85.31	70.20/82.79	62.74/90.42	<u>55.39/87.79</u>	<u>64.60/89.28</u>
<b>PLOOD</b>		<b>76.60/69.93</b>	<b>82.98/62.40</b>	<b>79.08/69.17</b>	<b>64.53/80.46</b>	<b>77.84/73.20</b>

Table 2: Performance comparisons of the **PLOOD** framework and **two existing PLL methods with five OOD scores** on the **five OOD datasets** of **CIFAR-100** under partial rate ( $p = 0.1$ ). **AUPR-IN(%)** and **FPR95(%)** are used for the evaluation. The underline indicates the optimal result of the current PLL method, and the bolded font is the optimal result of all cases.

Metrics		AUPR-IN ( $\uparrow$ ) / FPR95 ( $\downarrow$ )				
PLL methods	OOD scores	Fashion	LSUN	Tiny	DTD	Fooling
PaPi [16]	ODIN [10]	62.75/82.98	63.17/92.21	55.23/93.09	43.83/88.09	51.22/92.08
	DML [22]	60.18/84.61	62.57/77.96	63.97/80.44	41.52/92.46	50.55/96.86
	Entropy [3]	64.19/78.78	63.56/81.12	63.20/79.94	41.76/90.15	49.78/98.18
	Energy [12]	63.96/79.98	64.18/77.76	62.55/78.66	43.11/89.29	<u>52.43/88.85</u>
	J.Energy [15]	<u>64.69/78.08</u>	<u>65.30/75.64</u>	<u>65.16/76.20</u>	<u>44.24/87.45</u>	52.19/90.16
CAVL [20]	ODIN [10]	62.69/82.49	61.79/86.08	53.32/89.93	41.95/90.93	54.37/89.09
	DML [22]	62.72/80.68	62.97/80.38	59.97/82.77	35.83/94.89	53.27/88.56
	Entropy [3]	60.31/81.66	61.91/84.30	58.57/83.18	35.35/95.78	52.29/89.26
	Energy [12]	64.53/79.79	<u>64.41/80.01</u>	57.80/82.77	43.29/89.42	54.30/88.17
	J.Energy [15]	<u>65.54/77.82</u>	60.84/83.06	<u>61.07/80.23</u>	<u>46.03/87.59</u>	<u>54.76/87.41</u>
<b>PLOOD</b>		<b>73.49/68.33</b>	<b>72.38/69.62</b>	<b>71.31/71.36</b>	<b>51.46/81.43</b>	<b>61.71/80.42</b>

**Impacts of PE module on PLOOD with SSFE (SSFE+PE V.S. SSFE+other OOD scores):** to evaluate the impact of the PE module on PLOOD, we conducted experiments by combining the SSFE module in PLOOD with five other OOD metrics: ODIN, DML, Entropy, Energy, and J.Energy, which were compared with the PE method. The verification was carried out on three OOD datasets on CIFAR-100: Fashion, LSUN, and Tiny. The SSFE module was kept consistent across all OOD indicators. The results are presented in Figure 2. Our observations revealed that the AUPR-IN and FPR95 of the SSFE module on the other five OOD indicators were notably worse than those of the PE-based method. Particularly on the Fashion dataset, PE’s AUPR-In increased by almost 10% compared to the ODIN indicator, while FPR95 decreased by approximately 15%. In comparison to the other two Energy-based indicators, the PE module benefits from the labeling confidence learned by the SSFE module. This significantly reduces the possibility of inaccurate labeling during the training phase when evaluating in-distribution (ID) and OOD samples. Eliminating the impact of misweighting can enhance detection performance, improve the classification accuracy of ID samples, and reduce the detection error rate of OOD samples. Notably, that although the performance of the five OOD indicators based on SSFE modules is inferior to that of PE, it has seen significant improvement compared to those based on PaPi and CAVL. This further validates the effectiveness and superiority of the proposed framework PLOOD.

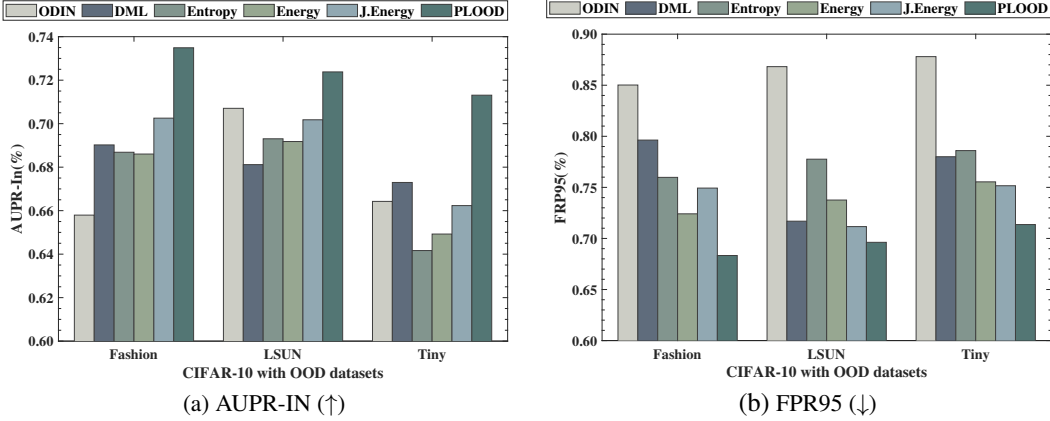


Figure 2: The results of the ablation experiment of the PE module on three OOD data sets of CIFAR-100. Use the SSFE module in PLOOD combined with other OOD indicators to compare with the proposed PE-based PLOOD.

Table 3: AUPR-IN(%) of the ablation experiments of the SSFE module on **CIFAR-10** (Comparisons between PaPi, CAVL with PE and PLOOD based on the SSFE module, respectively). (+\*) represents the improvement percentage of PE compared with Energy and J.Energy. And [-\*|-\*] indicates the percentage decrease of AUPR-IN in results of PaPi and CAVL without SSFE module.

	PaPi			CAVL			PLOOD[PaPi CAVL]
	PE	Energy	J.Energy	PE	Energy	J.Energy	
Fashion	71.04	67.14(+3.90)	68.98(+2.06)	70.43	65.38(+5.05)	62.64(+7.79)	76.60[-5.56 -6.17]
LSUN	78.19	75.08(+3.11)	76.65(+1.54)	78.28	74.47(+3.81)	70.20(+8.08)	82.98[-4.49 -4.70]
DTD	58.07	55.09(+2.98)	54.11(+3.96)	58.75	54.69(+4.06)	55.39(+3.36)	64.53[-6.46 -5.78]
Tiny	73.07	70.86(+2.21)	71.50(+1.57)	74.43	65.97(+8.46)	62.74(+11.7)	79.08[-6.01 -4.65]
Fooling	70.91	67.15(+3.76)	67.31(+3.60)	69.50	62.94(+6.56)	64.60(+4.90)	77.84[-6.93 -8.34]

**Impacts of SSFE module on PLOOD with PE (Comparisons among PaPi+PE, CAVL+PE, and SSFE+PE):** To further investigate the impact of the SSFE module on PLOOD, we conducted the following ablation experiment: a comparative analysis of SOTA’s two PLLs combined with PE and PLOOD (SSFE combined with PE). Since PaPi and CAVL do not provide the label confidence matrix required to generate PE with  $G_{LC}$ , we ensured fairness by generating the  $G_{LC}$  required in the PE module using the SSFE module in PLOOD. Our validation was performed on five OOD datasets of CIFAR-10. Additionally, we included a comparison between Energy and J.Energy as an auxiliary analysis. The results are presented in Tables 3 and 4. Our findings reveal that compared to PaPi and CAVL, the AUPR-In performance of PLOOD based on the SSFE module has improved by nearly 5% across the five datasets, while the FRP95 performance has shown an improvement of 2.6% to 11.9%. Particularly on the Fooling dataset, PLOOD exhibited an 7.30% and 11.9% improvement, respectively, compared to the other two PLL algorithms. These results demonstrate that the SSFE module in PLOOD has achieved superior performance compared to PaPi and CAVL without the ability to recognize the OOD samples, as it has learned features that can distinguish OOD negative samples. Furthermore, it is worth noting that our proposed PaPi and CAVL algorithms combined with PE indicators have significantly enhanced

Table 4: FRP95(%) of the ablation experiments of the SSFE module on **CIFAR-10** (Comparisons between PaPi, CAVL with PE and PLOOD based on the SSFE module, respectively). (+\*) represents the improvement percentage of PE compared with Energy and J.Energy. And [-\*|-\*] indicates the percentage increase FRP95 of in results of PaPi and CAVL without SSFE module.

	PaPi			CAVL			PLOOD[PaPi CAVL]
	PE	Energy	J.Energy	PE	Energy	J.Energy	
Fashion	72.79	77.12(-4.33)	75.48(-2.69)	72.82	80.46(-7.64)	85.31(-12.4)	69.93[+2.86 +2.89]
LSUN	68.24	73.76(-5.52)	72.08(-3.84)	74.36	79.01(-4.65)	82.79(-8.43)	62.40[+5.84 +11.9]
DTD	84.61	88.31(-3.70)	88.01(-4.40)	85.71	88.10(-2.39)	87.79(-2.08)	80.46[+4.15 +5.25]
Tiny	76.62	82.21(-5.59)	79.04(-2.42)	75.51	83.77(-8.26)	90.42(-14.9)	69.17[+7.45 +6.34]
Fooling	80.50	85.32(-4.82)	85.01(-4.51)	85.10	90.18(-5.08)	89.28(-4.18)	73.20[+7.30 +11.9]



OOD detection performance compared to existing Energy and J.Energy. This further validates that the framework of PLOOD proposed in this study offers substantial advantages in addressing the OODPLL problem.

## 4 Conclusion

This paper presents a new framework called PLOOD, which aims to tackle the issue of OODPLL task in open-set scenarios effectively. The framework comprises an SSFE module and a novel PE-based OOD detection module. The SSFE module leverages self-supervised learning to generate various rotated objects from training samples, providing emulated OOD samples and relative label confidence for PLL model training. In this way, the PLL model can learn distinguishable feature representations between ID and OOD samples. Moreover, the PE module utilizes the energy model framework along with the label confidence resulted from the SSFE module to address misidentification issue stemming from imprecise PLL labeling. Therefore, an effective guidance for PLL in OOD object detection is provided. Extensive experiments on CIFAR-10 and CIFAR-100 datasets illustrate that PLOOD notably enhances PLL models' performance and generalization capabilities, establishing a new benchmark for robustness and accuracy in open-world scenarios.

## References

- [1] Paul Albert, Eric Arazo, Noel E O'Connor, and Kevin McGuinness. Embedding contrastive unsupervised features to cluster in-and out-of-distribution noise in corrupted image datasets. In *European Conference on Computer Vision*, pages 402–419. Springer, 2022. 1
- [2] Jessa Bekker and Jesse Davis. Learning from positive and unlabeled data: A survey. *Machine Learning*, 109(4):719–760, 2020. 1
- [3] Robin Chan, Matthias Rottmann, and Hanno Gottschalk. Entropy maximization and meta classification for out-of-distribution detection in semantic segmentation. In *Proceedings of the IEEE/CVF International Conference on Computer Vision*, pages 5128–5137, 2021. 3.1, 1, 2
- [4] Shengzhuang Chen, Long-Kai Huang, Jonathan Richard Schwarz, Yilun Du, and Ying Wei. Secure out-of-distribution task generalization with energy-based models. *Advances in Neural Information Processing Systems*, 36, 2024. 1
- [5] Hsien-Tzu Cheng, Chun-Fu Yeh, Po-Chen Kuo, Andy Wei, Keng-Chi Liu, Mong-Chi Ko, Kuan-Hua Chao, Yu-Ching Peng, and Tyng-Luh Liu. Self-similarity student for partial label histopathology image segmentation. In *Computer Vision—ECCV 2020: 16th European Conference, Glasgow, UK, August 23–28, 2020, Proceedings, Part XXV 16*, pages 117–132. Springer, 2020. 1
- [6] Nanqing Dong, Michael Kampffmeyer, and Irina Voiculescu. Learning underrepresented classes from decentralized partially labeled medical images. In *Medical Image Computing and Computer Assisted Intervention - MICCAI 2022 - 25th International Conference, Singapore, September 18–22, 2022, Proceedings, Part VIII*, volume 13438 of *Lecture Notes in Computer Science*, pages 67–76. Springer, 2022. 1
- [7] Charles Elkan and Keith Noto. Learning classifiers from only positive and unlabeled data. In *Proceedings of the 14th ACM SIGKDD international conference on Knowledge discovery and data mining*, pages 213–220, 2008. 1, 2
- [8] Spyros Gidaris, Praveer Singh, and Nikos Komodakis. Unsupervised representation learning by predicting image rotations. In *International Conference on Learning Representations*, 2018. 1
- [9] Yuheng Jia, Fuchao Yang, and Yongqiang Dong. Partial label learning with dissimilarity propagation guided candidate label shrinkage. *Advances in Neural Information Processing Systems*, 36, 2024. 1
- [10] Shiyu Liang, Yixuan Li, and Rayadurgam Srikant. Enhancing the reliability of out-of-distribution image detection in neural networks. *arXiv preprint arXiv:1706.02690*, 2017. 3.1, 1, 2
- [11] Shuqi Liu, Yuzhou Cao, Qiaozhen Zhang, Lei Feng, and Bo An. Consistent complementary-label learning via order-preserving losses. In *International Conference on Artificial Intelligence and Statistics*, pages 8734–8748. PMLR, 2023. 1
- [12] Weitang Liu, Xiaoyun Wang, John Owens, and Yixuan Li. Energy-based out-of-distribution detection. *Advances in neural information processing systems*, 33:21464–21475, 2020. 1, 2.3, 2.3.2, 3.1, 1, 2
- [13] Jiaqi Lv, Biao Liu, Lei Feng, Ning Xu, Miao Xu, Bo An, Gang Niu, Xin Geng, and Masashi Sugiyama. On the robustness of average losses for partial-label learning. *IEEE Transactions on Pattern Analysis and Machine Intelligence*, 2023. 1

- [14] Sen Pei, Xin Zhang, Bin Fan, and Gaofeng Meng. Out-of-distribution detection with boundary aware learning. In *European Conference on Computer Vision*, pages 235–251. Springer, 2022. 1
- [15] Haoran Wang, Weitang Liu, Alex Bocchieri, and Yixuan Li. Can multi-label classification networks know what they don't know? *Advances in Neural Information Processing Systems*, 34:29074–29087, 2021. 1, 3.1, 1, 2
- [16] Shiyu Xia, Jiaqi Lv, Ning Xu, Gang Niu, and Xin Geng. Towards effective visual representations for partial-label learning. In *Proceedings of the IEEE/CVF Conference on Computer Vision and Pattern Recognition*, pages 15589–15598, 2023. 3.1, 1, 2
- [17] Ming-Kun Xie, Jiahao Xiao, Hao-Zhe Liu, Gang Niu, Masashi Sugiyama, and Sheng-Jun Huang. Class-distribution-aware pseudo-labeling for semi-supervised multi-label learning. *Advances in Neural Information Processing Systems*, 36, 2024. 1
- [18] Mingyu Xu, Zheng Lian, Lei Feng, Bin Liu, and Jianhua Tao. Alim: Adjusting label importance mechanism for noisy partial label learning. *Advances in Neural Information Processing Systems*, 36, 2024. 1
- [19] Jingkang Yang, Kaiyang Zhou, Yixuan Li, and Ziwei Liu. Generalized out-of-distribution detection: A survey. *arXiv preprint arXiv:2110.11334*, 2021. 1
- [20] Fei Zhang, Lei Feng, Bo Han, Tongliang Liu, Gang Niu, Tao Qin, and Masashi Sugiyama. Exploiting class activation value for partial-label learning. In *International conference on learning representations*, 2022. 3.1, 1, 2
- [21] Wenqiao Zhang, Changshuo Liu, Lingze Zeng, Beng Chin Ooi, Siliang Tang, and Yueting Zhuang. Learning in imperfect environment: Multi-label classification with long-tailed distribution and partial labels. In *IEEE/CVF International Conference on Computer Vision, ICCV 2023, Paris, France, October 1-6, 2023*, pages 1423–1432. IEEE, 2023. 1
- [22] Zihan Zhang and Xiang Xiang. Decoupling maxlogit for out-of-distribution detection. In *Proceedings of the IEEE/CVF Conference on Computer Vision and Pattern Recognition*, pages 3388–3397, 2023. 3.1, 1, 2
- [23] Haotian Zheng, Qizhou Wang, Zhen Fang, Xiaobo Xia, Feng Liu, Tongliang Liu, and Bo Han. Out-of-distribution detection learning with unreliable out-of-distribution sources. *Advances in Neural Information Processing Systems*, 36, 2024. 1